

# RSC Advances



This is an *Accepted Manuscript*, which has been through the Royal Society of Chemistry peer review process and has been accepted for publication.

*Accepted Manuscripts* are published online shortly after acceptance, before technical editing, formatting and proof reading. Using this free service, authors can make their results available to the community, in citable form, before we publish the edited article. This *Accepted Manuscript* will be replaced by the edited, formatted and paginated article as soon as this is available.

You can find more information about *Accepted Manuscripts* in the [Information for Authors](#).

Please note that technical editing may introduce minor changes to the text and/or graphics, which may alter content. The journal's standard [Terms & Conditions](#) and the [Ethical guidelines](#) still apply. In no event shall the Royal Society of Chemistry be held responsible for any errors or omissions in this *Accepted Manuscript* or any consequences arising from the use of any information it contains.

**AlCl<sub>3</sub> and liquid Al assisted extraction of Nd from NaCl-KCl melts via  
intermittent galvanostatic electrolysis**

Xing Li<sup>a</sup>, Yong-De Yan<sup>a,b,z</sup>, Mi-Lin Zhang<sup>a,z</sup>, Yun Xue<sup>b</sup>, Hao Tang<sup>a</sup>, De-Bin Ji<sup>a</sup>,  
Zhi-Jian Zhang<sup>b</sup>

*<sup>a</sup>Key Laboratory of Superlight Materials and Surface Technology, Ministry of Education, College of Materials Science and Chemical Engineering, Harbin Engineering University, Harbin 150001, China*

*<sup>b</sup>Key Discipline Laboratory of Nuclear Safety and Simulation Technology, Harbin Engineering University, Harbin 150001, China*

---

<sup>z</sup> Email: [y5d2006@hrbeu.edu.cn](mailto:y5d2006@hrbeu.edu.cn), [zhangmilin@hrbeu.edu.cn](mailto:zhangmilin@hrbeu.edu.cn)

**Abstract** The electrochemical reduction of Nd(III) was investigated on an inert W and a liquid Al electrode in molten NaCl–KCl eutectic salt. On both W and liquid Al electrodes, the reduction of Nd(III) ions to Nd(0) metal occurred in a single reaction step, which avoids the corrosion reaction:  $2\text{Nd(III)} + \text{Nd} \rightarrow 3\text{Nd(II)}$ . Therefore, corrosion of Nd metal in this molten chloride media is not expected. The co-reduction behavior of Nd(III) and Al(III) ions was studied on a W electrode in NaCl–KCl–AlCl<sub>3</sub>–NdCl<sub>3</sub> melts. Five kinds of Al–Nd intermetallic compounds were detected via cyclic voltammetry and open circuit chronopotentiometry. Intermittent galvanostatic electrolysis was employed on liquid Al electrodes to extract Nd in the form of Al–Nd alloys in NaCl–KCl–NdCl<sub>3</sub> melts. Nd, AlNd<sub>3</sub>, Al<sub>2</sub>Nd, and AlNd phases were identified by X-ray diffraction (XRD). With the increase of electrolytic time, the content of Nd-rich Al–Nd intermetallic compound in Al–Nd alloy increased. The morphology and micro-zone chemical analysis of the deposits were characterized by scanning electron microscopy (SEM) equipped with energy dispersive spectrometry (EDS), and Al<sub>11</sub>Nd<sub>3</sub> phase was confirmed by EDS analysis.

## Introduction

Nuclear energy provides a significant contribution to the overall energy supply. However, every year, the worldwide nuclear power plants generate a large quantity of nuclear waste, which is discharged from the used fuel and contains highly radioactive long-lived minor actinides (MA) and fission products (FPs). To significantly reduce volumes and radiotoxicity of the waste, the so-called partitioning and transmutation (P&T) techniques are being investigated in most countries with significant nuclear power generating capacity.<sup>1,2</sup> In this way, transuranium elements (TRU) recycled by separation from FPs (partitioning) and subsequently transmuted into stable or shorter-lived nuclides with the assistance of neutron (transmutation). This would greatly facilitate the disposal and management of wastes and raise public acceptance of nuclear energy.<sup>3</sup> Till now, two main reprocessing technologies have been widely studied: hydrometal-lurgical (aqueous) and pyrochemical (or non-aqueous) technologies. Compared with hydrometal-lurgical technology, advantages of pyrochemical reprocessing are higher levels of radiation tolerance, higher thermal and radiation stability towards heat generating FPs. Therefore, pyro-reprocessing technology based on electrometallurgy with molten salts as electrolyte is a more promising partitioning process. Special attention should be paid to rare earth elements (RE) because of their strong neutron absorption properties, which are the most awkward FPs to be separated from the TRU for their chemical similarity with the TRU.<sup>4,5</sup> On the other hand, there is a problem concerned with accumulation of FPs in the molten salts. When the concentration of FPs exceeds 10 wt% in the melts, it must

be regenerated to avoid affecting the TRU/FPs separation efficiency and to recycle the molten salts; because the accumulation of FPs in the solvent will modify their physical and chemical properties.<sup>5,6</sup>

Neodymium is one of major FPs elements with larger neutron capture cross sections, which is required to be removed from molten salts.<sup>7</sup> In molten fluoride, such as LiF–CaF<sub>2</sub>, LiF–NaF, LiF–CaCl<sub>2</sub>, and LiF melts,<sup>8–11</sup> Nd(III) is reduced to Nd(0) in a one-step process with three-electron transfer. Generally, in molten chloride, the reduction of Nd(III) takes place in two consecutive steps: Nd(III)+e<sup>-1</sup>→Nd(II), Nd(II)+2e<sup>-1</sup>→Nd(0), such as LiCl–CaCl<sub>2</sub>, LiCl–BaCl<sub>2</sub>, CaCl<sub>2</sub>–NaCl, and LiCl–KCl melts.<sup>12–16</sup> The corrosion reaction is expected: 2Nd(III)+Nd→3Nd(II), which is responsible for a low current yield in the electrolysis and a low stability of the deposits. Interestingly, Nohira et al. have found that in NaCl–KCl melts the Nd(III) reduction on an inert electrode is a one-step, three-electron exchange, reaction.<sup>17</sup> They have prepared different Nd–Ni alloys on Ni plate electrodes at various potentials. The formation reactions of the Nd–Ni alloys and their corresponding equilibrium potentials were determined. Eutectic NaCl–KCl melts with a melting point of 930 K was chosen as electrolyte due to its high thermal stability, the natural abundance of sodium and potassium, and the availability of a stable Ag<sup>+</sup>/Ag reference electrode.<sup>18</sup> Kuznetsov et al. have investigated redox electrochemistry and formal standard redox potentials of the Eu(III)/Eu(II) redox couple in NaCl–KCl melt.<sup>19</sup> The electrochemical behaviour of cerium oxychloride in MgCl<sub>2</sub>–NaCl–KCl ternary eutectic was investigated by cyclic voltammetry at 823 K.<sup>20</sup> Smolenskii et al. have studied

electrochemical behavior of cerium oxide ions in NaCl–KCl melt.<sup>21</sup> Picard and co-workers have studied the electrochemical properties of plutonium in NaCl–KCl eutectic salts.<sup>22</sup> These researchers obtained the thermodynamic data of Eu, Ce and Pu in NaCl–KCl melts, which is of crucial importance for the understanding of the separation process of FPs from TRU and the design of the separation cells.

Theoretical separation efficiency between the TRU and FPs from the molten salt is related to both the number of electrons exchanged to produce metal on the electrode and the potential gap ( $\Delta E$ ) between their reduction and the potential of the solvent.<sup>23</sup> As the reduction potential of neodymium is close to that of the common solvents, two methods can be used to increase  $\Delta E$ : (i) using a nobler metal (Al, Ni, Cu) than it as a cathode material leading to the formation of intermetallic compounds by shifting their reduction potentials towards more positive potentials, which is usually called underpotential electrodeposition; (ii) direct alloying with other metallic elements on inert electrodes by co-reduction.

Therefore, in this paper, we tried to study the Nd(III) reduction in NaCl–KCl melts not only on an inert W electrode with the assistance of  $\text{AlCl}_3$ , but also at a liquid Al electrode.

## **Experimental**

### **Preparation and purification of the melt**

The chloride eutectic NaCl–KCl (NaCl:KCl=50.6:49.4 mol%, analytical grade  $\geq 99.5\%$  and  $99.5\%$ , respectively ) placed in a alumina crucible was dried under vacuum for more than 72 h at 473 K to remove excess water before being used. Al(III)

and Nd(III) ions were introduced into NaCl–KCl melts in the form of anhydrous  $\text{AlCl}_3$  and  $\text{NdCl}_3$  (Aladdin Chemistry Co. Ltd  $\geq 99.95\%$ ), respectively. To remove oxide ions and the oxidation of  $\text{NdCl}_3$ , HCl was bubbled into the melt before each experiment. And then, Ar gas was bubbled into the melt to remove remanent HCl,  $\text{O}_2$  and  $\text{H}_2\text{O}$  to maintain an inert environment.

### **Electrochemical apparatus and electrodes**

Electrochemical tests, such as cyclic voltammetry, open circuit chronopotentiometry and galvanostatic electrolysis, were carried out using an Autolab PGSTAT 302N potentiostat/galvanostat controlled with the Nova 1.8 software package. The working electrodes were a polished W wire ( $d=1$  mm) and a liquid Al (about 2-3 g) placed in an alumina crucible ( $d=1.5$  cm,  $h=2.2$  cm). A W wire ( $d=1$  mm) placed in an alumina sleeve was immersed in the cathode Al and used as an electric lead. The working electrodes were cleaned by applying an anodic polarization between each measurement. The counter electrode was a spectral pure graphite rod ( $d=6$  mm). All the potentials in this study are given with respect to  $\text{Ag}^+/\text{Ag}$  couple, which consisted of  $\text{AgCl}$  (1.0 wt.%) in NaCl–KCl eutectic salt with a Ag-wire ( $d=0.5$  mm) inserting into a 3 mm diameter quartz tube.

### **Preparation and characterization of Al–Nd alloys**

Al–Nd alloys were prepared via intermittent galvanostatic electrolysis on liquid Al electrodes. In this way galvanostatic electrolysis was applied for a given time, and then it was interrupted for a given period to allow Nd diffusion into the liquid Al substrate. This process was repeated several times. After electrolysis, the samples

were washed with ethylene glycol to remove solidified salts attached on the surface of the alloy samples. To make a cross-section, the deposits were successively polished with 360#, 600#, 1500# and 2000# metallographic emery papers and abrasive finishing machine. The samples were analyzed by X-ray diffraction (XRD) (Rigaku D/max-TTR-III diffractometer) using Cu-K $\alpha$  radiation at 40 kV and 150 mA. Scanning electron microscopy (SEM) equipped with energy dispersive spectrometry (EDS) (JSM-6480A; JEOL Co., Ltd.) was used to analysis the microstructure and micro-zone chemical of bulk Al-Nd alloys.

## Results and discussion

### cyclic voltammetry

Fig. 1 shows the cyclic voltammograms obtained on a W and a liquid Al electrode in NaCl-KCl melts. The electrochemical window of the melt system on the liquid Al is limited by the reduction of Al(III) and Na(I) ions, which is much narrower than that on the W electrode. Interestingly, the intensities of the anodic signals related to the oxidation of Na on both W and Al electrodes are much lower than that of their corresponding reduction signals. This is due to the formation of Na fog and the high solubility of Na in NaCl melt.<sup>24</sup> On glassy carbon electrodes electrode, Kuznetsov et al. have obtained similar curves in NaCl-KCl melts.<sup>25</sup>

After the addition of Nd(III) in NaCl-KCl melts (Fig. 2), on the W electrode, a new pair of signals C/C' was detected. The signal C corresponds to the reduction of Nd(III) in NaCl-KCl melts in a single process:  $\text{Nd(III)} + 3\text{e}^{-1} \rightarrow \text{Nd(0)}$ .<sup>17</sup> The corresponding anodic signal C' is related to the oxidation of Nd metal. On the liquid Al electrode, the

reduction of Nd(III) (see signal I) occurs at about  $-1.0$  V via the formation of Al–Nd alloy:  $y\text{Nd(III)} + 3ye^{-1} + x\text{Al} \rightarrow \text{Al}_x\text{Nd}_y$ , whose potential is more positive than that on the W electrode. The reduction potential shifting toward anodic direction is attributed to a lowering of the activity coefficient of Nd in liquid Al phase. In general, the formation potential of Al–Nd alloy with higher Al content should be close to that of the deposition of Al. Therefore, signal I should be related with Al-rich Al–Nd alloy. Moreover, the deposition potential of Nd(III) on liquid Al electrode is much more positive than that of Na(I), which allows the electrochemical extraction of Nd into Al without the co-reduction of solvent.

Fig. 3 shows a series of cyclic voltammograms of NaCl–KCl–NdCl<sub>3</sub> melts obtained on a liquid Al electrode at different scan rates. The following information can be obtained from these curves: 1) the cathodic/anodic peak currents are directly proportional to the square root of the scan rates. This suggests that Nd(III) reduction/oxidation reaction is a diffusion-controlled process both in the melt and the metallic phases;<sup>26,27</sup> 2) the cathodic/anodic peak potentials change with the increase of scan rates, which indicates the system is not fully reversible; 3) the ratio of cathodic/anodic peak currents is close to one, indicating the diffusion coefficients of Nd(III) in the melt and the metallic phases are assumed to be similar.

To further study the formation of Al–Nd alloy, the co-reduction of Al(III) and Nd(III) in NaCl–KCl melts was investigated. Fig. 4 shows cyclic voltammograms obtained on a W electrode in NaCl–KCl–AlCl<sub>3</sub>–NdCl<sub>3</sub> melts at different cathodic limits. Five pairs of signals were detected. The signals A/A' peaked at about

$-0.88/-0.68$  V are attributed to the deposition/dissolution of Al(III) ions in NaCl–KCl melts. As seen from Fig. 2 the signal C' corresponding to the dissolution of Nd occurs at about  $-1.81$  V. Therefore, signal I', II', III', and IV' located between the dissolution of Al and Nd should correspond to the dissolution of four kinds of Al–Nd intermetallic compounds.<sup>28,29</sup> The corresponding cathodic signals I, II, III, and IV are related to the formation of Al–Nd intermetallic compounds, which are formed via the underpotential deposition of Nd(III) on pre-deposited Al coated W electrode. According to the phase diagram of Al and Nd,<sup>30</sup> at the experimental temperature, there exist five solid phases Al–Nd intermetallic compounds,  $\text{Al}_{11}\text{Nd}_3$ ,  $\text{Al}_3\text{Nd}$ ,  $\text{Al}_2\text{Nd}$ ,  $\text{AlNd}$ , and  $\text{AlNd}_2$ . Therefore, the  $\text{NdCl}_3$  concentration was adjusted to seek for more information about Al–Nd intermetallic compounds (see Fig. 5). Compared with the cyclic voltammograms in Fig. 4, a new signal (V') was detected in the anodic direction corresponding to the dissolution of an Nd rich Al–Nd alloy. Moreover, interestingly, the differences among the intensity of each anodic peak become larger, which is probably due to different formation rates of Al–Nd intermetallic compounds in the molten salt.

### **Open-circuit chronopotentiometry**

Open-circuit chronopotentiometry is an appropriate means to study the equilibrium potentials of intermetallic compounds. In this method, potentiostatic electrolysis was carried out to deposit a thin layer of specimen on a W electrode. Then, the open-circuit potential of the electrode is registered versus time in the melts. During this process, a potential plateau is observed when the composition of the electrode

surface is within the range of a two-phase coexisting state. Fig. 6 displays open circuit chronopotentiometry curves obtained on the W electrode in LiCl–KCl–AlCl<sub>3</sub> (2 wt.%)–NdCl<sub>3</sub> (2 wt.%) melts after potentiostatic electrolysis for different durations. Apart from potential plateau C corresponding to the equilibrium potentials of redox Nd/Nd(III), five potential plateaus (I, II, III, IV and V) were observed. With reference of the phase diagram of Al and Nd,<sup>30</sup> plateaus V, IV, III, II and I at about –1.44, –1.35, –1.27, –1.20 and –1.08 V are associated with two-phase coexisting states of 1) AlNd<sub>2</sub> and AlNd; 2) AlNd and Al<sub>2</sub>Nd; 3) Al<sub>2</sub>Nd and Al<sub>3</sub>Nd; 4) Al<sub>3</sub>Nd and Al<sub>11</sub>Nd<sub>3</sub>; 5) Al<sub>11</sub>Nd<sub>3</sub> and Al. Each plateau corresponding to the reaction is considered as follows:



The number of plateaus and their corresponding potentials are in agreement with the anodic peaks in the voltammograms in Fig.5.

### **Extraction of Nd and characterization of Al–Nd alloy**

Based on above electrochemical results, intermittent galvanostatic electrolysis was carried out on liquid Al electrodes to extract Nd in the form of Al–Nd alloys. Liquid Al placed in a small alumina crucible was used as the working electrode. After electrolysis, the alloy sample was kept in the melt with its gradually cooling. The NaCl–KCl salt was difficult to adhere on the surface of the crucible. Then, the

samples were separated from the salt and washed by ethylene glycol, and stored inside the glove box until their analysis.

Fig. 7 shows XRD patterns of Al–Nd alloy prepared at 1003 K at liquid Al electrodes in NaCl–KCl–NdCl<sub>3</sub> (4 wt.%) melts by galvanostatic electrolysis at 0.6 A for 2 h (sample A), 4 h (sample B), 6 h (sample C) and 8 h (sample D), respectively. In samples A, B, and C, Al, Nd, AlNd<sub>3</sub>, Al<sub>2</sub>Nd and AlNd phases were identified. The presence of Nd is precipitated out of the Al matrix during cooling period of the alloy after electrolysis due to its limited solubility in Al at room temperature. Al phase is predominant in samples A and B due to the liquid Al electrode. Moreover, there are some unknown diffraction peaks that could not be identified by current XRD database, which are thought to be related to other Al–Nd intermetallic compounds. In sample C, AlNd<sub>3</sub> phase is the predominance. However, only Al, Nd, AlNd<sub>3</sub> and AlNd phases were detected in sample D with predominance of AlNd<sub>3</sub>. Therefore, with the increase of electrolysis time, the content of Nd-rich Al–Nd intermetallic compound in Al–Nd alloy increases. Interestingly, the detected AlNd<sub>3</sub> phase in samples A, B, C and D is liquid at the experimental temperature,<sup>30</sup> which is formed during the cooling period of the alloy.

To study the distribution of Nd element in Al–Nd alloy, SEM and EDS analysis were employed. Fig. 8 shows cross-sectional SEM of samples A, B, C and D. The samples are composed of gray and bright zones. EDS results (see Fig. 9) of the points labeled 001, 002 and 003 taken from the gray and bright zones indicate that the deposit is composed of Al and Nd. Nd mainly distributes at the bright zones,

indicating that the bright zones are Al–Nd intermetallic compounds. The atom percentage ratios Al/Tm of points 001 and 002 are about 4.3 and 4.2, respectively. Therefore, the precipitated Al–Nd intermetallic compound is thought to be  $\text{Al}_{11}\text{Nd}_3$ . The ratios are a little higher than that of  $\text{Al}_{11}\text{Nd}_3$ , due, most likely, to the characteristic X-ray of Al overlapping with Nd. Since the current XRD data base lacks the JCPDS of  $\text{Al}_{11}\text{Nd}_3$  alloy, therefore, the unknown diffraction peaks in XRD patterns (in Fig. 7) might be related to the  $\text{Al}_{11}\text{Nd}_3$  phase.

Based on above results,  $\text{Al}_{11}\text{Nd}_3$ ,  $\text{Al}_2\text{Nd}$ ,  $\text{AlNd}$  and  $\text{AlNd}_3$  intermetallic compounds were detected in Al–Nd alloys. The reason of the absence of  $\text{Al}_3\text{Nd}$  and  $\text{AlNd}_2$  is that they are not stable phases in NaCl–KCl melts in liquid Al and easily change to other alloy phases or their formation rates are very slow.<sup>31,32</sup> In LiCl–KCl– $\text{AlCl}_3$ – $\text{NdCl}_3$  melts, only  $\text{Al}_3\text{Nd}$  and  $\text{Al}_2\text{Nd}$  phases were detected by Xu et al. in Al–Nd alloy obtained by galvanostatic electrolysis.<sup>16</sup> Massot et al. identified  $\text{Al}_{11}\text{Nd}_3$ ,  $\text{Al}_3\text{Nd}$ ,  $\text{AlNd}_2$  and  $\text{AlNd}_3$  intermetallic compounds in LiF– $\text{CaF}_2$ – $\text{AlF}_3$ – $\text{NdF}_3$  melts via potentiostatic electrolysis at different potentials.<sup>33</sup> The results suggest that all kind of intermetallic compounds are possible to form at the cathode. However, only the stable phases predominate in the deposits.

The ICP analyses of all samples obtained by galvanostatic electrolysis are listed in Table 1. The results show that the chemical compositions of alloys are consistent with the phase structures of the XRD patterns. When the electrolysis time is 2 h, the content of Nd in the alloy is low. Meanwhile, the current efficiency was also monitored. With the increase of electrolysis time, the current efficiency decreases.

which is related to the limited diffusion rate of Nd in Al phase. Most of deposited Nd formed Al-Nd intermetallic compounds which conserve Nd. While, some lost in the molten salt during electrolysis.

### Conclusion

In NaCl–KCl molten salt, the reduction of Nd(III) ions to Nd(0) metal occurred in a single reaction step on both W and liquid Al electrodes. The Nd(III) ions reduction potential on a liquid Al electrode is much more positive than that on a W electrode. The co-reduction of Al and Nd in NaCl–KCl–AlCl<sub>3</sub>–NdCl<sub>3</sub> melts was studied on a W electrode by cyclic voltammetry and open circuit chronopotentiometry. Five kinds of Al–Nd intermetallic compounds at about –1.44, –1.35, –1.27, –1.20 and –1.08 V were detected. Extraction of Nd was carried out via intermittent galvanostatic electrolysis at 0.6 A at liquid Al electrodes. Nd, AlNd<sub>3</sub>, Al<sub>2</sub>Nd, and AlNd phases were identified by XRD in the deposits and Al<sub>11</sub>Nd<sub>3</sub> phase was confirmed by EDS analysis. During electrolysis, the corrosion reaction is not expected: 2Nd(III)+Nd→3Nd(II). Therefore, NaCl–KCl melt is suitable for extraction of Nd.

### Acknowledgments

The work was financially supported by the High Technology Research and Development Program of China (No. 2011AA03A409), the National Natural Science Foundation of China (21103033, 21101040, and 91226201), the Fundamental Research funds for the Central Universities (HEUCF201403001), the Foundation for University Key Teacher of Heilongjiang Province of China and Harbin Engineering

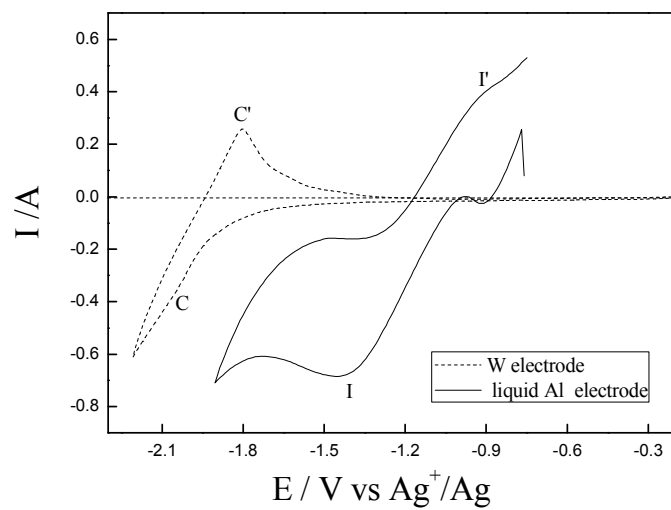
University (1253G016 and HEUCFQ1415), and the Special Foundation of China and Heilongjiang Postdoctoral Science Foundation (2013T60344 and LBH-TZ0411).

## References

- 1 L. Koch, J.-P. Glatz, R. J. M. Konings, J. Magill, *ITU Annual Report*, 1999, EUR19054.
- 2 J. Magill, V. Berthou, D. Haas, J. Galy, R. Schenkel, H.-W. Wiese, G. Heusener, J. Tommasi and G. Youinou, *Nuclear Energy*, 2003, **42**, 263–277.
- 3 Y. Castrillejo, C. de la Fuente, M. Vega, F. de la Rosa, R. Pardo, E. Barrado, *Electrochim. Acta*, 2013, **97**, 120–131.
- 4 T. Wakabayashi, *Progress in Nuclear Energy*, 2002, **40**, 457–463.
- 5 Y. Castrillejo, A. Vega, M. Vega, P. Hernández, J.A. Rodríguez, E. Barrado, *Electrochim. Acta*, 2014, **118**, 58–66.
- 6 D. Hudry, I. Bardez, A. Rakhnatullin, C. Bessada, F. Bart, S. Jobic, P. Deniard, *J. Nucl. Mater.*, 2008, **381**, 284–289.
- 7 K. Fukasawa, A. Uehara, T. Nagai, T. Fujii, H. Yamana, *J. Nucl. Mater.*, 2011, **414**, 265–269.
- 8 P. Taxil, L. Massot, C. Nourry, M. Gibilaro, P. Chamelot, L. Cassayre, *J. Fluorine Chem.*, 2009, **130**, 94–101.
- 9 C. Hamel, P. Camelot, P. Taxil, *Electrochim. Acta*, 2004, **49**, 4467–4476.
- 10 E. Stefanidaki, C. Hasiotis, C. Kontoyannis, *Electrochim. Acta*, 2001, **46**, 2665–2670.
- 11 C. Nourry, L. Massot, P. Chamelot, P. Taxil, *J. Appl. Electrochem.*, 2009, **39**, 927–933.

- 12 G. De Córdoba, A. Laplace, O. Conocar, J. Lacquement, C. Caravaca, *Electrochim. Acta*, 2008, **54**, 280-288.
- 13 K. Fukasawa, A. Uehara, T. Nagai, T. Fujii, H. Yamana, *J. Alloys Compd.*, 2011, **509**, 5112–5118.
- 14 K. Fukasawa, A. Uehara, T. Nagai, T. Fujii, H. Yamana, *J. Nucl. Mater.*, 2011, **414**, 265–269.
- 15 P. Masset, R.J.M. Konings, R. Malmbeck, J. Serp, J.P. Glatz, *J. Nucl. Mater.*, 2005, **344**, 173–179.
- 16 Y.D. Yan, Y.L. Xu, M.L. Zhang, Y. Xue, W. Han, Y. Huang, Q. Chen, Z.J. Zhang, *J. Nucl. Mater.*, 2013, **433**, 152–159.
- 17 K. Yasuda, S. Kobayashi, T. Nohira, R. Hagiwara, *Electrochim. Acta*, 2013, **92**, 349–355.
- 18 K. Yasuda, S. Kobayashi, T. Nohira, R. Hagiwara, *Electrochim. Acta*, 2013, **106**, 293–300.
- 19 S.A. Kuznetsov, M. Gaune-Escard, *Electrochim. Acta*, 2001, **46**, 1101–1111.
- 20 S. Ghosh, S. Vandarkuzhali, P. Venkatesh, G. Seenivasan, T. Subramanian, B. P. Reddy, K. Nagarajan, *Electrochim. Acta*, 2006, **52**, 1206–1212.
- 21 V.V. Smolenskii, E.V. Komarov, N.P. Borodina, V.S. Mityaev, L.G. Khrustova, A.L. Bove, A.V. Bychkov, M.V. Kormilitsyn, *Radiochemistry*, 1999, **41**, 430.
- 22 D. Lambertin, S. Ched'homme, G. Bourgès, S. Sanchez, G. Picard, *J. Nucl. Mater.*, 2005, **341**, 124–130.

- 23 P. Chamelot, L. Massot, C. Hamel, C. Nourry, P. Taxil, *J. Nucl. Mater.*, 2007, **360**, 64–74.
- 24 X. Li, Y.D. Yan, M.L. Zhang, Y. Xue, W. Han, H. Tang, Z.P. Zhou, X.N. Yang, and Z.J. Zhang, *J. Electrochem. Soc.*, 2014, **161(1)**, D48–D54.
- 25 S.A. Kuznetsov, M. Gaune-Escard, *Electrochim. Acta*, 2001, **46**, 1101–1111.
- 26 G. De Córdoba, A. Laplace, O. Conocar, J. Lacquement, C. Caravaca, *Electrochim. Acta*, 2008, **54**, 280–288.
- 27 G. De Córdoba, A. Laplace, O. Conocar, J. Lacquement, *J. Nucl. Mater.*, 2009, **393**, 459–464.
- 28 M. Gibilaro, L. Massot, P. Chamelot, P. Taxil, *Electrochim. Acta*, 2009, **54**, 5300–5306.
- 29 H. Wendt, K. Reuhl, V. Schwarz, *Electrochim. Acta*, 1992, **37 (2)**, 237
- 30 T.B. Massalski, J.L. Murray, L.H. Bennett, H. Baker, Binary alloy Phase Diagrams, American Society for Metals, 1990.
- 31 T. Iida, T. Nohira, Y. Ito, *Electrochim. Acta*, 2001, **46**, 2537–2544.
- 32 V. Smolenski, A. Novoselova, *Electrochim. Acta*, 2012, **63**, 179–184.
- 33 M. Gibilaro, L. Massot, P. Chamelot, P. Taxil, *J. Nucl. Mater.*, 2008, **382**, 39–45.



A comparison of the cyclic voltammograms obtained on the W (dotted line) and liquid Al (solid line) electrodes in NaCl-KCl-NdCl<sub>3</sub> (2 wt.%) melt. Temperature: 1003 K, scan rate: 0.1 V s<sup>-1</sup>.